HHS Public Access

Author manuscript

*Biochim Biophys Acta Biomembr*. Author manuscript; available in PMC 2020 May 01.

Published in final edited form as:

*Biochim Biophys Acta Biomembr*. 2019 May 01; 1861(5): 1030–1036. doi:10.1016/j.bbamem.2019.03.005.

# Calcium-induced transformation of cardiolipin nanodisks

**Colin A. Fox**[1], **Patricia Ellison**[1], **Nikita Ikon**[2], and **Robert O. Ryan**[1,*]

[1]Department of Biochemistry and Molecular Biology University of Nevada, Reno, Reno, NV 89557

[2]Department of Nutritional Sciences and Toxicology University of California, Berkeley, Berkeley CA

## Abstract

Miniature membranes comprised of tetramyristoylcardiolipin (CL) and apolipoprotein (apo) A-I, termed nanodisks (ND), are stable, aqueous soluble, reconstituted high density lipoproteins. When CL ND, but not dimyristoylphosphatidylcholine (PC) ND, were incubated with $CaCl_2$, a concentration dependent increase in sample turbidity occurred, consistent with CL undergoing a bilayer to non-bilayer transition. To assess the cation specificity of this reaction, CL ND were incubated with various mono- and divalent cations. Whereas monovalent cations had no discernable effect, $MgCl_2$ and $SrCl_2$ induced a response similar to $CaCl_2$. When ND were formulated using different weight ratios of CL and PC, those possessing 100% CL or 75% CL remained susceptible to $CaCl_2$ induced sample turbidity development while ND possessing 50% CL displayed reduced susceptibility. ND comprised of 25 % CL and 75 % PC were unaffected by $CaCl_2$ under these conditions. SDS PAGE analysis of insoluble material generated by incubation of CL ND with $CaCl_2$ revealed that nearly all apoA-I was recovered in the insoluble fraction along with CL. One h after addition of EDTA to $CaCl_2$-treated CL ND, sample clarity was restored. Collectively, the data are consistent with a model wherein $Ca^{2+}$ forms a bidentate interaction with anionic phosphates in the polar head group of CL. As phosphate group repositioning occurs to maximize $Ca^{2+}$ binding, CL acyl chains reposition, accentuating the conical shape of CL to an extent that is incompatible with the ND bilayer structure.

### Keywords

Cardiolipin; nanodisk; calcium; apolipoprotein A-I; bilayer; hexagonal II phase

## Introduction

Cardiolipin (CL) is a uniquely structured glycerophospholipid that localizes to the inner membrane of mitochondria [1]. Unlike other phospholipids, cardiolipin possesses two phosphates, three glycerols and four fatty acyl chains. Due to its relatively small polar head

*Address correspondence to: Robert O. Ryan, robertryan@unr.edu, Biochemistry and Molecular Biology University of Nevada, Reno, Mail Stop 0330, 1664 N. Virginia Street, Reno, NV 89557 .

group and four esterified fatty acids, CL possesses a “cone-shaped” molecular structure [2,3]. As a result, CL is considered to be a “non-bilayer” phospholipid that, when present in a bilayer setting, exerts negative curvature pressure [4]. Whereas CL is not well accommodated in planar bilayer membranes [5], it is a key component of highly curved bilayers such as the cristae membranes of mitochondria [6].

Calcium plays an important role in mitochondrial signaling and function [7]. Mitochondrial calcium overload is known to induce apoptosis and it is conceivable that interactions between calcium, CL and cytochrome c are involved in molecular events that trigger apoptosis [8,9,10]. Interaction of calcium with CL containing liposomes is known to induce a bilayer to non-bilayer transition, resulting in formation of an inverted hexagonal II lipid phase [11,12,13]. The molecular basis for this phenomenon is not fully understood and, to date, most studies have been performed using liposomes that possess varying percentages (typically ~20%) of their phospholipid mass as CL [14,15,16]. One of the limitations associated with liposomes as a model system is the fact that up to one half of the bilayer phospholipid content resides in the inner monolayer leaflet where it is largely inaccessible to the external environment. In the case of multilamellar vesicles, an even greater proportion of liposomal phospholipid is inaccessible. Additionally, liposomes often display polydispersity, exhibit limited stability and scatter light to varying degrees, indicating a lack of complete solubility [17,18,19].

By contrast, recent studies have shown that CL can be fully solubilized in aqueous buffer upon incorporation into nanoscale membrane complexes comprised solely of CL and apolipoprotein (apo) A-I [20]. These complexes, termed nanodisks (ND), exist as disk-shaped phospholipid bilayers whose perimeter is circumscribed by an amphipathic scaffold protein, such as apoA-I [21]. Although CL is generally unstable in a planar bilayer setting, the apolipoprotein scaffold appears to exert a stabilizing force, effectively serving as a “belt” around the perimeter of the discoidal bilayer. Compared to liposomes, CL ND have inherent advantages for studies of molecular interactions, including a uniform nanoscale particle size distribution, complete aqueous solubility, ease of formulation, the absence of an inaccessible bilayer leaflet and, most remarkably, ND can be generated using CL as the sole lipid component. In the present study, CL ND were employed as a model system to investigate the effect of $CaCl_2$ on CL ND structure, stability and aqueous solubility.

## Materials and Methods

### Nanodisk formulation

Dimyristoylphosphatidylcholine (PC), tetramyristoyl cardiolipin (CL) and tetralinoleoyl cardiolipin were purchased from Avanti Polar Lipids. Unless otherwise indicated, studies reported herein employed tetramyristoyl CL. Five mg aliquots were dissolved in 200 μL CHCl3:CH3OH (3:1 v/v), and dried under a stream of $N_2$ gas, creating a thin film on the walls of the vessel. Samples were lyophilized overnight to remove residual solvent. To formulate ND, 750 μL 20 mM HEPES buffer, pH 7.2, was added to a 5 mg aliquot of dried phospholipid. The sample was vortexed to disperse the phospholipid which ultimately appeared as an opaque suspension. Subsequently, 2 mg recombinant human apoA-I [22] in 500 μL HEPES buffer was added to the lipid suspension. The final volume of the mixture

was 1.25 ml. PC ND were formulated by bath sonication of the PC/apoA-I mixture at 25 °C until the solution cleared (< 10 min). Tetramyristoyl CL ND (hereafter referred to as CL ND) were formulated in a similar manner, with the exception that bath sonication was performed at 48 °C. Tetralinoleoyl CL ND were formulated by bath sonication at 25 °C under an $N_2$ atmosphere.

### Gel filtration chromatography of ND samples

ND samples, formulated as above, were centrifuged at 14,000 × g for 2 min prior to gel permeation chromatography on a Superose 6 Increase 10/300 GL column using a GE AKTA Pure FPLC instrument. Two hundred μL ND (corresponding to 0.8 mg CL), were applied to the column. Samples were chromatographed in 20 mM HEPES at a flow rate of 0.5 ml/min with absorbance monitored at 280 nm and collection of 1.0 ml fractions.

### Incubation of ND with cations

Following formulation of ND, 25 μL aliquots (100 μg phospholipid; corresponding to 78 nmol CL or 147 nmol PC) were added to the wells of a UV Star microtiter plate (Greiner Bio-One). Indicated amounts of $CaCl_2$ were added to the wells. The final volume of all wells was maintained at 200 μL through addition of HEPES buffer. After addition of HEPES and $CaCl_2$, samples were incubated for 1 h at 22 °C or 37 °. Sample turbidity was measured as absorbance at 325 nm using a Spectramax M5 microplate reader. Background absorbance at 325 nm, determined in wells containing deionized water, was <0.05. To determine the effect of other cations, ND were added to a microtiter plate as described above. The chloride salt of specified mono- or divalent cations were added to the wells, samples incubated for 1 h at 22 °C and absorbance measured at 325 nm (i.e. turbidity). To assess partitioning of the apoA-I scaffold protein following $CaCl_2$-induced CL ND sample turbidity development, 25 μL CL ND (equivalent to 78 nmol CL) were incubated with 2000 nmol $CaCl_2$ in a final volume of 200 μL for 1 h at 22 °C. The turbid sample was centrifuged at 14,000 × g for 2 min to pellet insoluble material. The supernatant was recovered and the pellet re-suspended in 200 μl HEPES buffer. Ten μL aliquots of the supernatant and resuspended pellet were electrophoresed on a 4–20% SDS PAGE slab gel and stained with GelCode Blue Stain Reagent (Thermo). Gel images were documented on a GE Healthcare Typhoon Trio Variable Mode Imager. To assess the relative distribution of apoA-I in $CaCl_2$ disrupted CL ND supernatant and pellet fractions, densitometric analysis of gel band intensity was performed using ImageJ software [23]. To measure the relative distribution of CL between pellet and supernatant fractions generated by incubation of CL ND with $CaCl_2$, the CL specific fluorescent dye, 10-N-nonyl acridine orange [24] (Thermo) was employed. Samples were excited at 499 nm and emission monitored from 530 nm to 610 nm on a Spectramax M5 microplate reader in a fluorescence compatible microtiter plate (Greiner Bio-One).

### Incubation of mixed phospholipid ND with $CaCl_2$

To assess the effect of $CaCl_2$ on mixed phospholipid ND, different weight ratios of CL and PC were used to formulate “mixed lipid” ND. HEPES buffer (750 μl) was added to separate 5 mg aliquots of CL and PC followed by vortexing to hydrate the lipids. Aliquots of these PC and CL dispersions were combined to achieve the indicated phospholipid weight ratios. ApoA-I was then added to the mixed lipid dispersions at a 5:2 (w/w) lipid:protein ratio. ND

formation, as measured by sample clarification, was achieved by bath sonication at 48 °C for 2 min, alternating with bath sonication at 25 °C until sample absorbance was <0.07 at 325 nm (<10 min). For incubations with $CaCl_2$, aliquots of mixed lipid ND, containing 78 nmol CL, were added to the wells of a microtiter plate. Indicated amounts of $CaCl_2$ in HEPES buffer were added to each well (final volume 200 μL) and the plate incubated for 1 h at 22 °C prior to sample absorbance measurements.

### CL ND incubation with $CaCl_2$ and EDTA

CL ND were added to the wells of a microtiter plate as above. $CaCl_2$ (0 nmol, 600 nmol or 2000 nmol) was added and the samples incubated at 22 °C for 1 h. Following incubation, a 1:1 molar equivalent of EDTA to $CaCl_2$ was added to each sample. Total sample volumes after EDTA addition were maintained at 300 μL through addition of HEPES buffer. Samples were incubated for a further 1 h at 22 °C followed by absorbance measurement at 325 nm. In other experiments, EDTA-treated, $CaCl_2$-modified CL ND were analyzed by gel filtration chromatography as described above before and after bath sonication at 48 °C for 3 min and centrifugation at 14,000 × g for 2 min.

### Statistical Analysis

Statistical analyses were performed by two-way ANOVA followed by Dunnett's test to compare treated samples against control samples (Figures 2, 3, 4). Alternatively, the Holm-Sidak multiple t-test was used to compare the absorbance of $CaCl_2$ treated samples to $CaCl_2$ + EDTA treated samples (Figure 5a). Statistical tests were performed using GraphPad Prism version 8.02 for Windows (GraphPad Software, San Diego, CA)

## Results

### Cardiolipin ND formulation and model structure.

When aqueous dispersions of CL are incubated with apoA-I and subjected to bath sonication, lipid nanoparticle complex (i.e. ND) formation is evident by complete sample clarification [20]. Previous studies, using PC and other glycerophospholipids, revealed that ND exist as disk-shaped phospholipid bilayers whose perimeter is stabilized by interaction with apoA-I, an amphipathic α-helix-rich scaffold protein [21]. Unlike other glycerophospholipids that form ND, CL possesses a relatively small polar head group and four hydrophobic acyl chains, conferring a distinct cone-shaped structure to this lipid. Consistent with this, CL induces negative curvature pressure on bilayer membranes and is prone to adopting a non-bilayer state. With regard to the apparent ability of CL to form ND, it is conceivable that the apoA-I scaffold exerts a belt-like stabilizing force around the ND bilayer perimeter, as depicted in Figure 1A. In keeping with this model, FPLC gel filtration chromatography of CL ND (Figure 1B) reveals a homogenous population of particles in a similar size range to well characterized PC ND [25]. Thus, it may be considered that the scaffold function of apoA-I provides an opposing force to CL's tendency to transition to a non-bilayer state, thereby maintaining CL in a soluble bilayer state as ND.

### The effect of $CaCl_2$ on ND sample turbidity.

Both CL ND and PC ND are fully soluble in aqueous buffer. Negligible material precipitates upon centrifugation and samples remain stable for 1 week or more when stored at 4 °C. To determine the effect of $CaCl_2$ on ND structural integrity, PC ND and CL ND samples were incubated with increasing quantities of $CaCl_2$ for 1 h (Figure 2). In control incubations containing HEPES buffer alone, $CaCl_2$ had no effect on sample absorbance at 325 nm. Likewise, when PC ND were incubated with $CaCl_2$, little or no change in sample absorbance occurred. By contrast, CL ND undergo a marked $CaCl_2$ concentration dependent increase in sample turbidity. The rate of this reaction was temperature dependent, with turbidity development occurring more rapidly at 37 °C than at 22 °C. Moreover, the physiologically relevant CL molecular species, tetralinoleoyl CL is capable for forming ND [20] and is also susceptible to $CaCl_2$ induced ND disruption (data not shown). As seen in Figure 2, $CaCl_2$ levels below 400 nmol had little or no effect on CL ND sample turbidity. At 400 nmol $CaCl_2$, however, the sample became turbid and absorbance increased. As the amount of $CaCl_2$ was increased further, sample absorbance also increased, plateauing at 1000 nmol $CaCl_2$ / 78 nmol CL.

### Effect of alternate cations on CL ND sample turbidity.

To assess the cation specificity of the reaction induced by incubation with $CaCl_2$, CL ND (78 nmol CL) were incubated with increasing amounts of mono- or divalent cations (Figure 3). CL ND in buffer alone served as control and, in the absence of added cations, remained fully soluble. Addition of $CaCl_2$ induced the expected concentration-dependent increase in CL ND sample absorbance and a similar trend was observed with $MgCl_2$ and $SrCl_2$. The monovalent cations, NaCl and KCl, had no effect on CL ND sample turbidity.

### Effect of $CaCl_2$ on mixed phospholipid ND.

To further explore $CaCl_2$ mediated effects on CL ND, different weight ratios of CL and PC were used to formulate ND. The resulting mixed phospholipid ND were incubated with $CaCl_2$. ND comprised of 100% CL, 75% CL, 50% CL and 25% CL were incubated in the absence or presence of 2 fixed amounts of $CaCl_2$ for 1 h, followed by measurement of sample turbidity (Figure 4). The final CL content in each incubation was 100 μg (78 nmol). Similar to ND formulated with 100% CL, ND formulated at a 75:25 (w/w) ratio of CL to PC showed a strong $CaCl_2$ concentration-dependent increase in sample turbidity. ND formulated with a 50:50 (w/w) mixture of CL and PC showed a slight, but statistically significant, increase in absorbance at the highest $CaCl_2$ level tested. ND containing 25% CL and 75% PC were unaffected by incubation with $CaCl_2$ under these experimental conditions.

### Effect of EDTA on $CaCl_2$-induced CL ND sample turbidity.

To determine whether chelation of added calcium by EDTA is able to reverse $CaCl_2$-mediated effects on CL ND, samples of CL ND were incubated with $CaCl_2$ for 1 h to induce turbidity development. EDTA was then added (1:1 molar equivalence to $CaCl_2$) and the samples incubated for an additional 1 h, followed by absorbance determination at 325 nm (Figure 5A). CL ND incubated with 600 nmol $CaCl_2$, followed by 600 nmol EDTA, rapidly clarified. Samples treated with 2000 nmol $CaCl_2$ clarified more slowly upon addition of

EDTA, returning to near original absorbance by the end of the 1 h incubation period. FPLC gel filtration analysis of $CaCl_2$-treated CL ND samples clarified by incubation with EDTA revealed a slight increase in particle heterogeneity and centrifugation of this sample generated a small but reproducible precipitate (data not shown). However, bath sonication of EDTA clarified, $CaCl_2$-treated CL ND did not give rise to a precipitate upon centrifugation and FPLC gel filtration chromatography **(**Figure 5B**)** revealed a uniform population of particles whose elution characteristics were nearly indistinguishable from those of CL ND prior to incubation with $CaCl_2$.

### Effect of $CaCl_2$ on the interaction of apoA-I with CL.

According to the model presented in Figure 1, apoA-I is an essential structural component of CL ND. To determine whether apoA-I maintains contact with CL following incubation with $CaCl_2$, insoluble material formed during this reaction was pelleted by centrifugation and the supernatant removed. Following re-suspension of pelleted material in a volume of buffer equal to the reserved supernatant, aliquots of each were subjected to SDS PAGE (Figure 6). Densitometric scanning of the stained gel indicated >90 % of the apoA-I in the original CL ND sample was recovered in the insoluble fraction generated by incubation of CL ND with $CaCl_2$. Analysis of the relative distribution of CL between the supernatant and pellet fractions using an assay based on binding of 10-N-nonyl acridine orange to CL indicated >70 % of the CL was recovered in the pellet with <30 % in the supernatant. Taken together, the data indicate that, following $CaCl_2$-induced transition of CL to an insoluble, non-bilayer state, apoA-I remains associated with the lipid.

## Discussion

CL is a uniquely structured glycerophospholipid that plays an important role in mitochondrial structure and bioenergetics. CL is a cone-shaped lipid, owing to a relatively small polar head group and four fatty acyl chains. Consistent with this molecular shape, CL exerts negative curvature pressure on membranes and is prone to adopt a nonbilayer, inverted hexagonal II phase. Despite this tendency, CL not only exists stably in mixed lipid membranes but can be induced to form an apparent nanoscale size planar bilayer when an aqueous dispersion of this lipid is bath sonicated in the presence of isolated recombinant human apoA-I. The complexes formed are fully soluble in neutral pH buffer, stable for extended periods when stored at 4 °C and, based on gel filtration chromatography, display a homogeneous particle size distribution. These complexes, comprised solely of CL and apoA-I, termed CL ND, represent a novel miniature membrane system to investigate CL's interactome.

One example of a CL binding partner is calcium. Upon incubation with $CaCl_2$, fully soluble CL ND undergo a marked increase in sample turbidity, consistent with CL undergoing a transition from bilayer to non-bilayer state. This transition does not occur when PC ND are incubated with $CaCl_2$. The reaction is $CaCl_2$ concentration dependent and changes in sample turbidity are detectable at a ~1:5 molar ratio of CL to $CaCl_2$, while maximum sample absorbance values plateau at ã1:12 molar ratio of CL to $CaCl_2$. Mixed lipid ND that contain different ratios of CL and PC respond differently to $CaCl_2$. The response is directly related

to the CL content of the ND. Reducing the amount of CL in a given ND by replacing it with PC confers resistance against $CaCl_2$-induced transformation of ND from a soluble bilayer state to an insoluble non-bilayer state. Overall, these results reveal that decreasing the proportion of CL in ND decreases the absorbance increase induced by incubation with $CaCl_2$. In other words, mixed lipid ND containing a lower proportion of CL per ND require more $CaCl_2$ to induce a bilayer to non-bilayer transition. This trend holds for ND formulated to possess 100%, 75%, 50% and 25% CL content.

The reaction described between CL ND and $CaCl_2$ also occurs when CL ND are incubated with other divalent cations, including $MgCl_2$ and $SrCl_2$. Magnesium, which has the smallest atomic radius of the divalent cations tested, induced a lesser increase in sample absorbance than either calcium or strontium at the lower ion level tested. At higher amounts, however, all three divalent cations induced a similar increase in sample absorbance. On the other hand, incubation with monovalent cations across a wide concentration range had no discernable effect on CL ND. The specificity of this reaction for divalent cations suggests that the two negatively charged phosphate groups in CL's polar head group play a key role. Divalent cations, such as $Ca^{2+}$, are capable of forming a bidentate binding interaction with these phosphates, as depicted in Figure 7. Moreover, it is anticipated that, as the two phosphates reposition to increase contact with the $Ca^{2+}$ ion, conformational strain is placed on other parts of the CL molecule. This strain may be relieved by repositioning the hydrocarbon tails of CL in a manner that further accentuates its cone shape. Such a change in the orientation of CL hydrocarbon tails, relative to the polar head group, is postulated to accentuate the conical shape of CL, decreasing its ability to stably reside in planar bilayer structure of ND. It is likely such a molecular shape change, induced by calcium binding, ultimately leads to disruption of the ND bilayer structure and the transition of CL from a soluble bilayer to an insoluble non-bilayer state that ultimately precipitates from solution. This calcium-induced bilayer disruption may relate to other biological interactions in the CL interactome. In particular, release of cytochrome c from the inner mitochondrial membrane may be related to an influx of calcium into the mitochondria, though the exact mechanism remains under investigation [26, 27]. In any event, CL ND may be a viable model for examining this interaction in a controlled, readily accessible *in vitro* setting.

Whereas it is considered that the apolipoprotein scaffold surrounding the disk-shaped bilayer of ND exerts a stabilizing force that "holds" CL in a bilayer phase through direct contact of its amphipathic α-helices with otherwise exposed fatty acyl chains around the edge of the discoidal bilayer (see Figure 1), the data indicate calcium-mediated effects on CL structure exert an opposing force that, above a certain threshold, results in CL ND particle disruption. Based on experiments conducted with mixed phospholipid ND, as the CL content of a given ND formulation is increased, the easier it is for the stabilizing influence of the apolipoprotein to be exceeded by incubation with $CaCl_2$.

Once the scaffold protein's stabilizing force is exceeded, CL undergoes a bilayer to non-bilayer transition and this process coincides with obvious changes in sample turbidity. Remarkably, however, upon addition of EDTA, which effectively chelates all calcium present, including that bound to CL, an environment is created wherein apoA-I is capable of re-solubilizing CL, presumably by reconstitution of CL ND. FPLC analysis revealed that

bath sonication of EDTA clarified, $CaCl_2$-treated CL ND gives rise to an elution profile that is nearly indistinguishable from that of the starting CL ND. The observation that the reaction induced by $CaCl_2$ can be reversed by the addition of EDTA may be related to the fact that, following $CaCl_2$ mediated disruption of CL ND, apoA-I remains associated with the insoluble CL precipitate. Assuming $Ca^{2+}$ bound CL adopts a hexagonal II phase, then it is likely that apoA-I maintains a binding interaction with exposed hydrocarbon tails at the aqueous interface of this insoluble lipid phase, thereby minimizing contact between hydrophobic CL fatty acyl chains and the aqueous milieu, as depicted in Figure 8. Maintenance of a binding interaction between apoA-I and CL in the $CaCl_2$ disrupted state is likely a key factor in the ability of EDTA to promote re-formation of intact CL ND. Just as the initial formation of CL ND required bath sonication to generate a uniform homogenous population of CL ND, following EDTA treatment of $CaCl_2$ disrupted CL ND, bath sonication yielded a single major population of CL ND.

It is noteworthy that the major CL molecular species found in mitochondria of heart and muscle tissue is tetralinoleoyl CL. This molecular species is generated by acyl chain remodeling of nascent CL through the action of a transacylase termed tafazzin [28]. Although the potential benefits of establishing a uniform fatty acyl distribution in CL are not known, it has been shown that tafazzin activity *in vitro* is optimal when CL exists in a non-bilayer state [29]. Insofar as tetralinoleoyl CL is capable of forming ND and is susceptible to $CaCl_2$ mediated conversion to a non-bilayer state, this system may provide a model for understanding the role(s) of calcium in CL remodeling and its role in maintenance of mitochondrial membrane integrity.

## Acknowledgements

This work was supported by a grant from the National Institutes of Health (R37 HL64159). The authors thank Sharon Young, Irina Romenskaia, Jennifer Shearer and Mohamad Dandan for contributing to the development of this research.

## Abbreviations

| | |
|---|---|
| **CL** | Tetramyristoylcardiolipin |
| **PC** | Dimyristoylphosphatidylcholine |
| **ND** | Nanodisk |
| **ApoAI** | Apolipoprotein A-I |

## References

[1]. Horvath SE, Daum G (2013) Lipids of mitochondria, Prog. Lipid Res 52, 590–614. [PubMed: 24007978]

[2]. Cullis PR, de Kruijff B (1979) Lipid Polymorphism and the functional roles of lipids in biological membranes. Biochim Biophys Acta 559, 399–420. [PubMed: 391283]

[3]. Stepanyants N, Macdonald PJ, Francy CA, Mears JA, Qi X, Ramachandran R (2015) Cardiolipin's propensity for phase transition and its reorganization by dynamin-related protein 1 form a basis for mitochondrial membrane fission. Mol Biol Cell. 26, 3104–3116. [PubMed: 26157169]

[4]. Renner LD, Weibel DB (2011) Cardiolipin microdomains localize to negatively curved regions of E. coli membranes. Proc. Natl. Acad. Sci. U.S.A 108, 6264–6269. [PubMed: 21444798]

[5]. Lewis R, McElhaney RN (2009) The physicochemical properties of cardiolipin bilayers and cardiolipin-containing lipid membranes. Biochim Biophys Acta 1788, 2069–2079. [PubMed: 19328771]

[6]. Ikon N, Ryan RO (2017) Cardiolipin and mitochondrial cristae organization. Biochim Biophys Acta 1859, 1156–1163.

[7]. Brookes PS, Yoon Y, Robotham JL, Anders MW, Sheu SS (2004) Calcium, ATP, and ROS: a mitochondrial love-hate triangle. Am J Physiol Cell Physiol. 287, C817–C833. [PubMed: 15355853]

[8]. Paradies G, Petrosillo G, Paradies V, Ruggiero FM (2009) Role of cardiolipin peroxidation and $Ca^{2+}$ in mitochondrial dysfunction and disease. Cell Calcium. 45, 643–650. [PubMed: 19368971]

[9]. Celsi F, Pizzo P, Brini M, Leo S, Fotino C, Pinton P, Rizzuto R (2009) Mitochondria, calcium, and cell death: A deadly triad in neurodegeneration. Biochim Biophys Acta Bioenerg. 1787(5), 335–344.

[10]. Peng T, Jou MJ (2010) Oxidative stress caused by mitochondrial calcium overload. Ann N Y Acad Sci. 1201, 183–188. [PubMed: 20649555]

[11]. Rand RP, Sengupta S (1972) Cardiolipin forms hexagonal structures with divalent cations. Biochim Biophys Acta. 255, 484–492. [PubMed: 4333431]

[12]. De Kruijff B, Verkleij AJ, Leunissen-Bijvelt J, Van Echteld CJA, Hille J, Rijnbout H (1982) Further aspects of the calcium dependent polymorphism of bovine heart cardiolipin. Biochim Biophys Acta 693, 1–12. [PubMed: 7150583]

[13]. Kirk GL, Gruner SM, Stein DL (1984) A thermodynamic model of the lamellar to inverse hexagonal phase transition of lipid membrane-water systems. Biochemistry 23 1093–1102.

[14]. Cullis PR, Verkleij AJ, Ververgaert PHJ (1978) Polymorphic phase behaviour of cardiolipin as detected by $^{31}P$ NMR and freeze-fracture techniques. Effects of calcium, dibucaine and chlorpromazine. Biochim Biophys Acta 513, 11–20. [PubMed: 102344]

[15]. Smaal EB Schreuder C, van Baal JB, Tijburg PNM, Mandersloot JG, Kruijff BD, Gier JD (1987) Calcium-induced changes in permeability of dioleoylphosphatidylcholine model membranes containing bovine heart cardiolipin. Biochim Biophys Acta. 897, 191–196. [PubMed: 3099844]

[16]. Macdonald PM, Seelig J (1987) Calcium binding to mixed cardiolipinphosphatidylcholine bilayers as studied by deuterium nuclear magnetic resonance. Biochemistry. 26, 6292–6298. [PubMed: 3689777]

[17]. Sharma A, Sharma US (1997) Liposomes in drug delivery: progress and limitations. Int J Pharmaceut. 154, 123–140.

[18]. Akbarzadeh A, Rezaei-Sadabady R, Davaran S, Joo SW, Zarghami N, Hanifehpour Y, Samiei M, Kouhi M, Nejati-Koshki K (2013) Liposome: classification, preparation, and applications. Nanoscale Res Lett. 8, 102. [PubMed: 23432972]

[19]. Bozzuto F, Molinari A (2015) Liposomes as nanomedical devices. Int J Nanomedicine. 10, 975–999. [PubMed: 25678787]

[20]. Ikon N, Su B, Hsu F, Forte TM, Ryan RO (2015) Exogenous cardiolipin localizes to mitochondria and prevents TAZ knockdown-induced apoptosis in myeloid progenitor cells. Biochem Biophys Res Comm 464, 580–585. [PubMed: 26164234]

[21]. Ryan RO (2010) Nanobiotechnology applications of reconstituted high density lipoprotein. J. Nanobiotech 8, 8–28.

[22]. Ryan RO, Forte TM, Oda MN (2003) Optimized bacterial expression of human apolipoprotein A-I. Protein Expr Purif. 27, 98–103. [PubMed: 12509990]

[23]. Rueden CT, Schindelin J, Hiner MC, DeZonia BE, Walter AE, Arena ET, Eliceiri KW (2017) ImageJ2: ImageJ for the next generation of scientific image data. BMC Bioinformatics 18, 529. [PubMed: 29187165]

[24]. Garcia Fernandez MI, Ceccarelli D, Muscatello U (2004) Use of the fluorescent dye 10-N-nonyl acridine orange in quantitative and location assays of cardiolipin: a study of different experimental models. Anal Biochem. 328, 174–80. [PubMed: 15113694]

[25]. Wadsater M, Maric S, Simonsen JB, Mortensen K, Cardenas M (2013) The effect of using binary mixtures of zwitterionic and charged lipids on nanodisc formation and stability. Soft Matter. 9, 2329–2337.

[26]. Prudent J, McBride HM (2017) The mitochondria-endoplasmic reticulum contact sites: a signaling platform for cell death. Curr Opin Cell Biol. 47, 52–63. [PubMed: 28391089]

[27]. Giorgi C, Baldassari F, Bononi A, Bonora M, Marchi ED, Marchi S, Missiroli S, Patergnani S, Rimessi A, Suski JM, Wieckowsky MR, Pinton P (2012) Mitochondrial $Ca^{2+}$ and apoptosis. Cell Calcium 52, 36–43. [PubMed: 22480931]

[28]. Schlame M (2013) Cardiolipin remodeling and the function of tafazzin. Biochim Biophys Acta. 1831, 582–588. [PubMed: 23200781]

[29]. Schlame M, Acehan D, Berno B, Xu Y, Valvo S, Ren M, Stokes DL, Epand RM (2012) The physical state of lipid substrates provides transacylation specificity for tafazzin. Nat Chem Biol. 8, 862–869. [PubMed: 22941046]

## Highlights

- Cardiolipin nanodisks (CL ND) are stable, aqueous soluble nanoparticles
- $CaCl_2$ induces a transition of CL ND from bilayer to insoluble, non-bilayer state
- EDTA reverses the effects of $Ca^{2+}$, restoring CL ND structure and solubility
- Bidentate binding of $Ca^{2+}$ to CL phosphates induces a structural alteration
- The ND scaffold protein remains associated with precipitated $CaCl_2$ treated CL ND

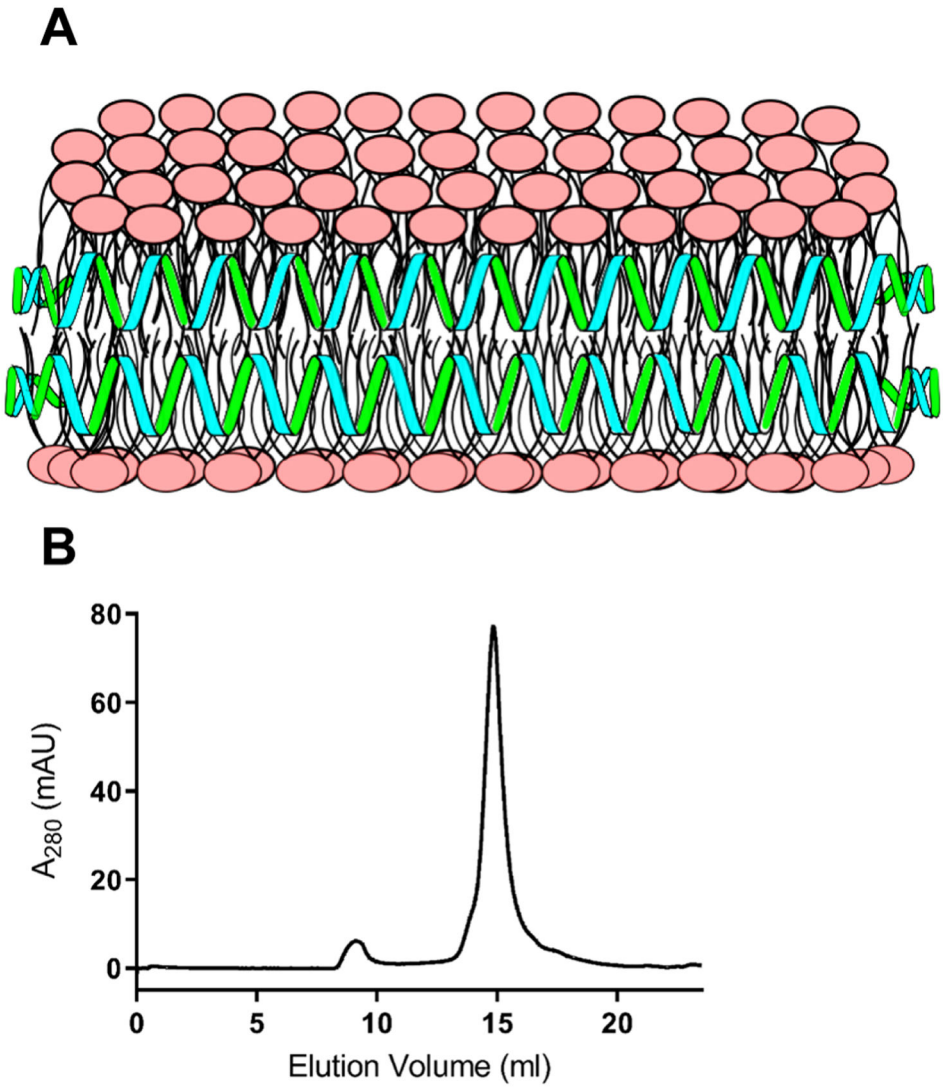


**Figure 1: Model structure of CL ND.**

**A**) In this depiction, CL (polar head groups in pink) is organized as a disk-shaped bilayer whose perimeter is circumscribed and stabilized by apoA-I (green/blue helices), which interacts with CL fatty acyl chains at the edge of the disk. **B**) FPLC size exclusion chromatography profile of CL ND. ND were formulated with apoA-I and CL as described. An aliquot of CL ND (0.32 mg apoA-I / 0.8 mg CL) in 20 mM HEPES buffer, pH 7.2, was applied to a Superose 6 Increase 10/300 GL column and elution monitored at 280 nm.

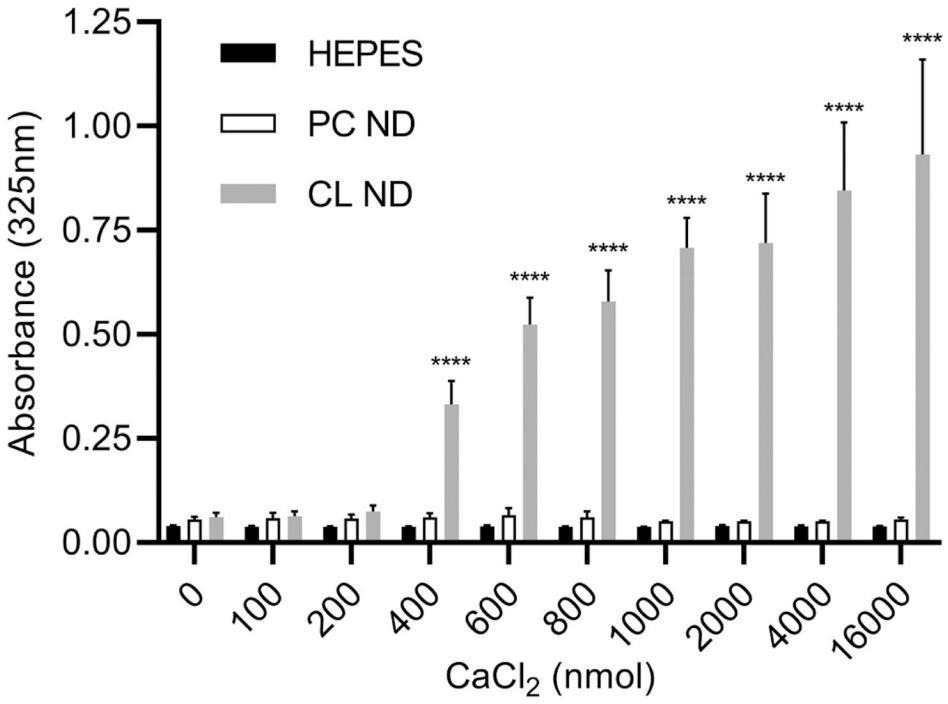


**Figure 2. Effect of $CaCl_2$ on ND sample integrity.**

ApoA-I containing PC ND and CL ND were formulated in HEPES buffer as described and aliquots of each (corresponding to 78 nmol CL or 147 nmol PC) were applied to the wells of a 96 well microtiter plate. To each well, indicated amounts of $CaCl_2$ (in HEPES buffer) were added and the volume adjusted to 200 μl with HEPES buffer. The plate was incubated for 1 h at 22 °C and, following incubation, sample absorbance measured at 325 nm on a SpectraMax plater reader. Values reported are the mean ± standard error (n = 9) ****, P<0.0001 versus HEPES control and PC ND.

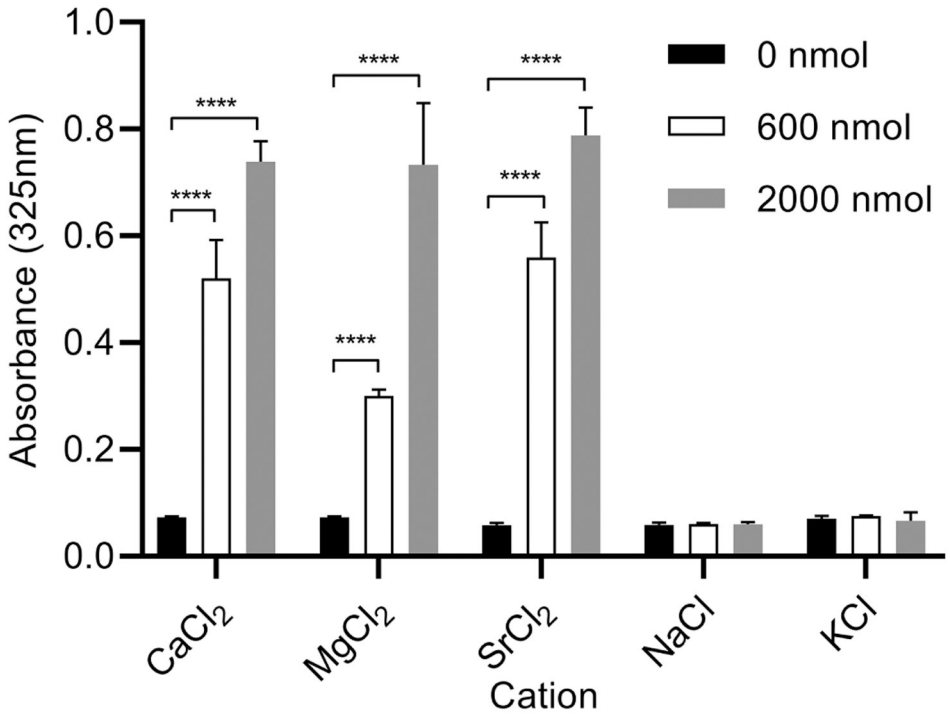


**Figure 3. Effect of alternate cations on ND sample integrity.**

Aliquots of CL ND (78 nmol CL), solubilized in HEPES buffer, were applied to the wells of a 96 well microtiter plate. To each well, specified quantities of the chloride salt of mono- or divalent cations was added and the volume adjusted to 200 μl with HEPES buffer. The plate was incubated for 1 h at 22 °C followed by sample absorbance determination at 325 nm. Values reported are the mean ± standard error (n = 3) ****, P<0.0001 versus 0 nmol divalent cation.

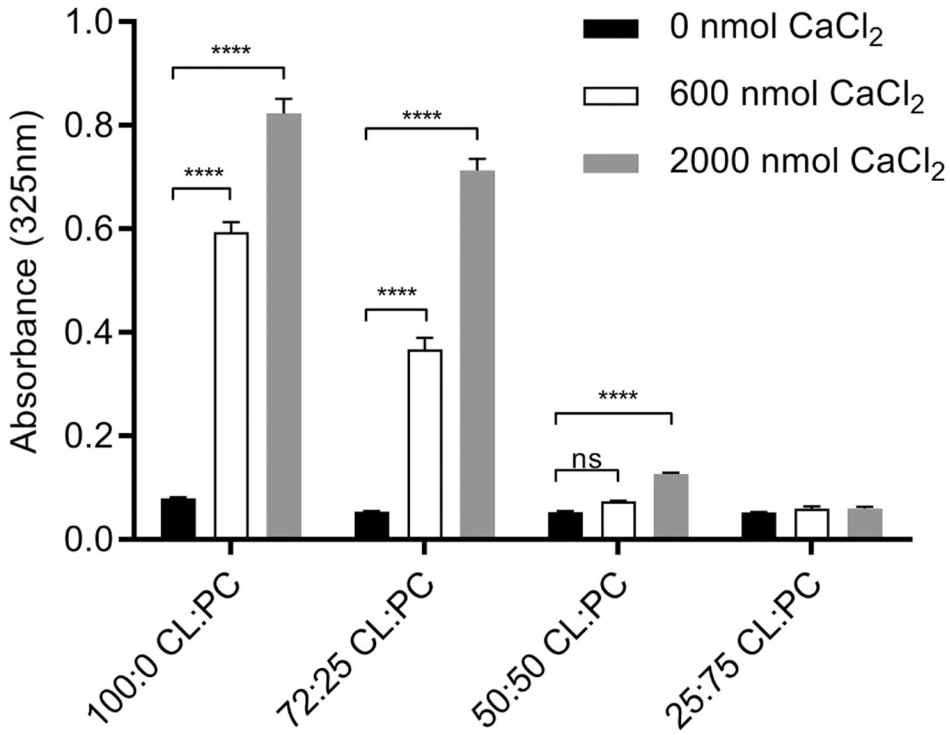


**Figure 4. Effect of calcium on mixed lipid ND sample integrity.**

ND containing specified weight ratios of CL and PC were formulated with apoA-I in HEPES buffer. Aliquots of the different ND samples (corresponding to 78 nmol CL), were added to the wells of a 96 well microtiter plate. To each well, indicated amounts of $CaCl_2$ were added and the volume adjusted to 200 μl with HEPES buffer. The plate was incubated for 1 h at 22 °C and, following incubation, sample absorbance at 325 nm was measured. Values reported are the mean ± standard error (n = 3) ****, $P<0.0001$ versus 0 nmol $CaCl_2$. ns, not significant.

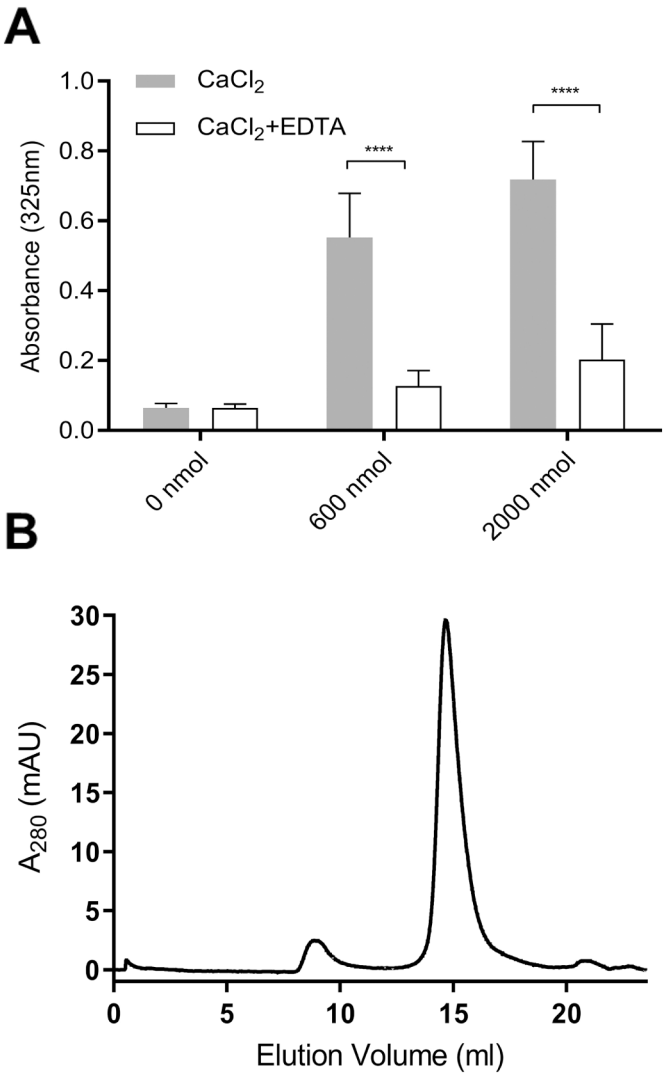


**Figure 5. Effect of EDTA on $CaCl_2$-disrupted CL ND.**

**A**) CL ND were formulated in HEPES buffer with apoA-I and aliquots corresponding to 78 nmol CL applied to the wells of a 96 well microtiter plate. Indicated amounts of $CaCl_2$ were added and the volume adjusted to 200 μl with HEPES buffer. The plate was incubated for 1 h at 22 °C and, following incubation, sample absorbance at 325 nm was measured on a Spectramax plate reader. Subsequently, EDTA, dissolved in HEPES buffer, was added to each well to achieve a concentration equivalent to that of the added $CaCl_2$. The final volume of each well was adjusted to 300 μl and the plate incubated for an additional 1 h at 22 °C. Following incubation, sample absorbance at 325 nm was measured. Values reported are the mean ± standard error (n = 6) ****, P<0.0001 calcium-treated versus EDTA-treated. **B)** FPLC size exclusion chromatography of EDTA-treated, $CaCl_2$-disrupted CL ND. A sample of CL ND (622 nmol CL), solubilized in HEPES buffer, was incubated with 8,000 nmol $CaCl_2$ for 1 h at 22 °C to induce sample turbidity development. To this sample, 8,000 nmol EDTA was added followed by incubation for 1 h at 22 °C to induce sample clarification. The

clarified sample was bath sonicated at 48 °C for 2 min followed by chromatography on a Superose 6 Increase 10/300 GL FPLC column with elution monitored at 280 nm.

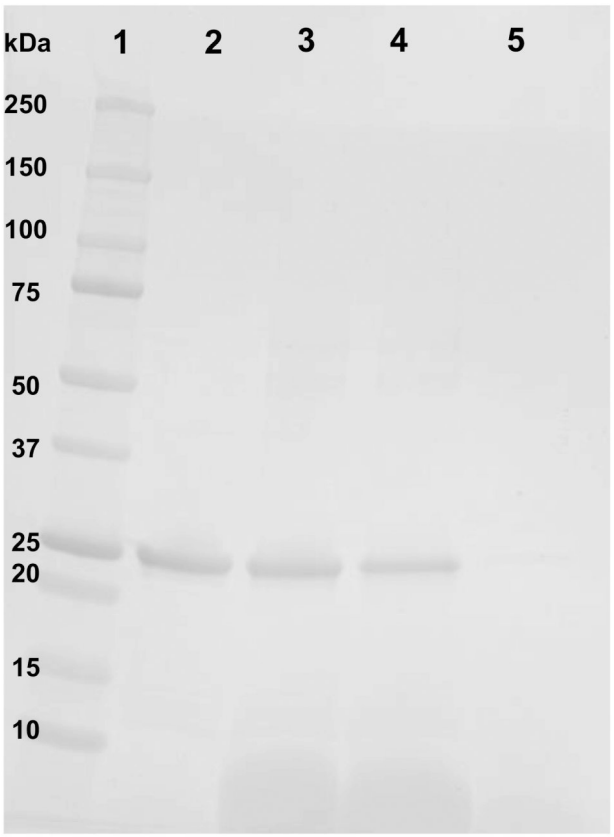


**Figure 6. Effect of $CaCl_2$-mediated disruption of CL ND on apoA-I solubility.**

CL ND were formulated with apoA-I in HEPES buffer and an aliquot, corresponding to 78 nmol CL, was incubated with 2000 nmol $CaCl_2$ for 1 h at 22 °C to induce sample turbidity development. Following this, the sample was centrifuged at 14,000 × g for 2 min and the supernatant recovered. The precipitate was re-suspended in a volume of HEPES buffer equal to that of the reserved supernatant. Equivalent aliquots of the resuspended pellet and supernatant were electrophoresed on a 4–20% acrylamide gradient SDS PAGE gel and stained with GelCode Blue. Lane 1) molecular weight markers; Lane 2) apoA-I standard; Lane 3) control CL ND; Lane 4) $CaCl_2$-disrupted CL ND re-suspended pellet; Lane 5) $CaCl_2$-disrupted CL ND supernatant.

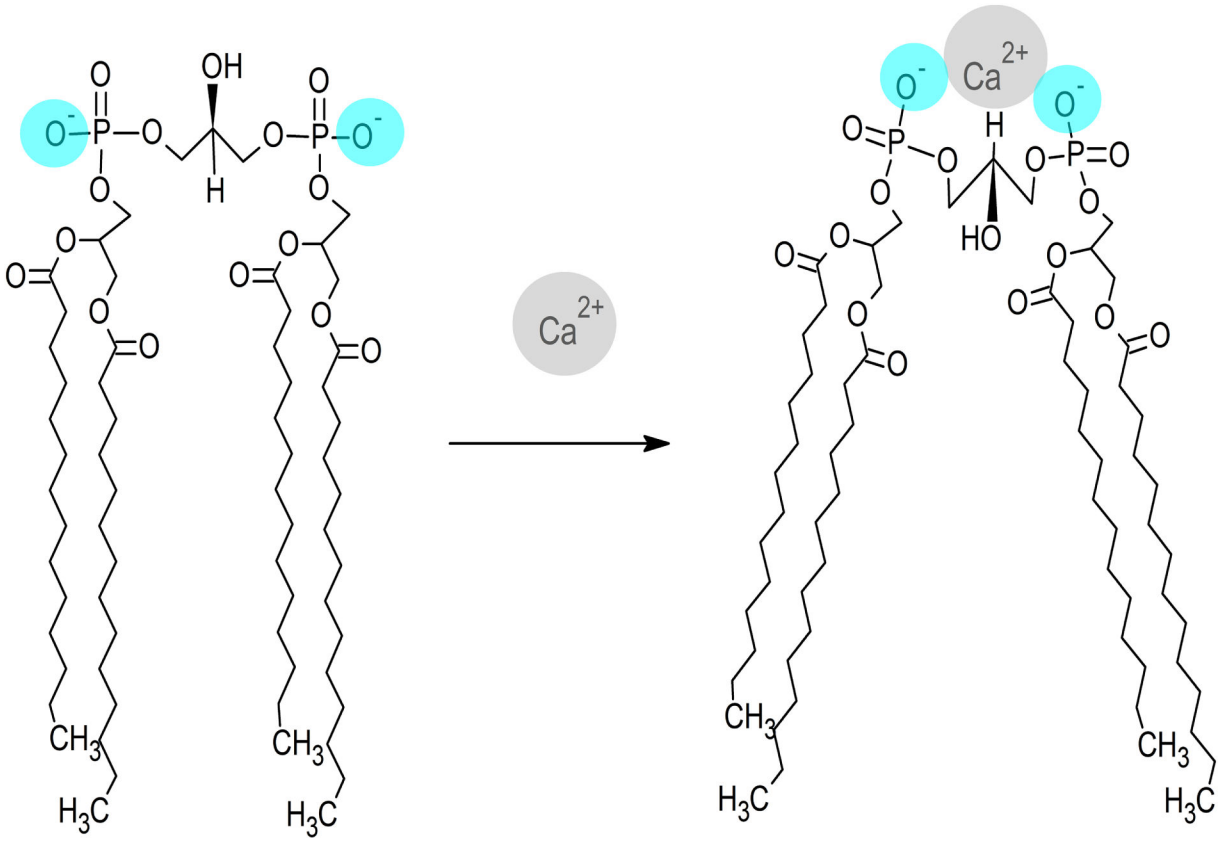


**Figure 7. Model depicting the effect of calcium binding on CL structure.**

Divalent cations, such as $Ca^{2+}$, are attracted to the anionic polar head group of CL, forming a bidentate binding interaction with its two phosphate moieties (blue). A single calcium ion localized between these phosphates induces structural repositioning of CL in order to maximize interaction with calcium. As the phosphate moieties converge toward the calcium ion, conformational strain is relieved by realignment of the CL fatty acyl chains, which results in the adoption of a conformation that is incompatible with a bilayer state.

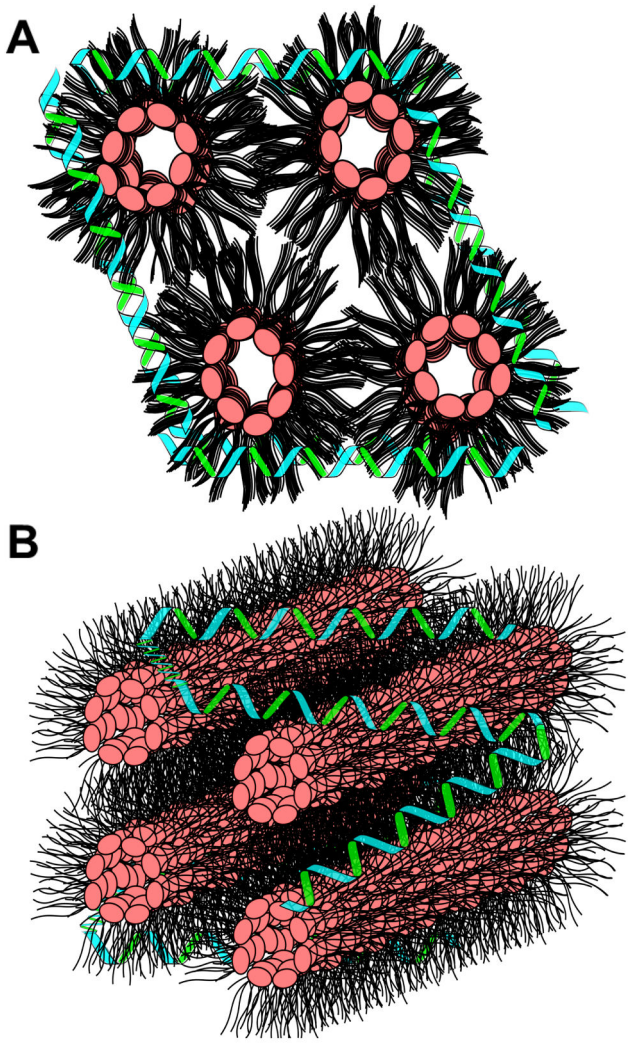


**Figure 8. Model of $CaCl_2$-disrupted CL ND.**

After addition of $CaCl_2$ to CL ND, CL molecules transition to a non-bilayer state, presumably an inverted hexagonal II phase. In an inverted hexagonal II phase, the CL polar head groups (pink) align toward the center of lipid cylinders while CL fatty acyl chains (black) project into the aqueous milieu. Data presented indicates apoA-I (green/blue helices) remains associated with CL following $CaCl_2$-mediated CL ND disruption. This association most likely involves apoA-I binding to exposed CL hydrocarbon tails, thereby providing some measure of protection from direct lipid interaction with the aqueous milieu. Upper image) End on depiction of CL in an inverted hexagonal II phase with apoA-I interacting with exposed acyl chains. Lower image) CL hexagonal II phase cylinders with associated apoA-I.